Journal of Applied Mechanics and Technical Physics, Vol. 49, No. 2, pp. 313–322, 2008

NUMERICAL MODELLING OF THE STABILITY OF LOADED SHELLS OF REVOLUTION CONTAINING FLUID FLOWS

S. A. Bochkarev and V. P. Matveenko

UDC 539.3

A mixed finite-element algorithm is proposed to study the dynamic behavior of loaded shells of revolution containing a stationary or moving compressible fluid. The behavior of the fluid is described by potential theory, whose equations are reduced to integral form using the Galerkin method. The dynamics of the shell is analyzed with the use of the variational principle of possible displacements, which includes the linearized Bernoulli equation for calculating the hydrodynamic pressure exerted on the shell by the fluid. The solution of the problem reduces to the calculation and analysis of the eigenvalues of the coupled system of equations. As an example, the effect of hydrostatic pressure on the dynamic behavior of shells of revolution containing a moving fluid is studied under various boundary conditions.

Key words: *shell theory, compressible fluid, potential theory, divergence, flutter.*

Introduction. Fluid flow at a considerable velocity can lead to static (divergence) or dynamic (flutter) instability of the pipe–fluid system. In turn, a static load [axial extension (compression) or hydrostatic (external) pressure] can also result in static instability of an elastic thin-walled body. Therefore, the joint action of hydrodynamic and static loads can have a stabilizing or destabilizing influence on the system considered, by increasing or decreasing the critical velocities of the fluid flow.

In theoretical studies (analytical and numerical), an elastic pipe is modeled as a circular beam [1], a shell of revolution [2–5] or a three-dimensional body [6]. The internal fluid flow is described using potential theory [2–5] or Euler equations [6].

The finite-element method provides great capabilities for modeling the dynamic behavior of pipe–moving fluid systems from a point of view of choosing possible tools for describing elastic bodies and fluid flows [4–6]. However, there have been a few theoretical studies exploring the influence of static loads on the dynamic characteristics of pipe–moving fluid systems. The influence of axial compression and hydrostatic pressure was considered in [5]. An analytical expression for the pressure of a moving incompressible fluid was obtained with the framework of potential theory using the method of separation of variables, and the characteristic parameters included in the expression were determined from the Sanders shell equations written in the form of the Lamé equations. In [6], the influence of hydrostatic pressure was studied using a finite-element algorithm in which a cylindrical shell is described by the three-dimensional theory of elasticity and the hydrodynamic pressure is determined from the Euler equations with dynamic boundary conditions taking into account the fluid flow.

In the present paper, a mixed finite-element algorithm is proposed to study the influence of a static load on the dynamic characteristics of a pipe–moving fluid system. This algorithm integrates a system of equations for the fluid obtained by applying the Galerkin method to the equations of potential theory and the shell equations obtained using the principle of possible displacements. The preliminary stress state is determined by solving the static problem.

Institutes of Mechanics of Continuous Media, Ural Division, Russian Academy of Sciences, Perm' 614013; bochkarev@icmm.ru; mvp@icmm.ru. Translated from Prikladnaya Mekhanika i Tekhnicheskaya Fizika, Vol. 49, No. 2, pp. 185–195, March–April, 2008. Original article submitted April 17, 2007.

1. Formulation of the Problem. Equations of Motion for Shells of Revolution. We consider an elastic shell of revolution of length L and thickness h with the smallest radius R. The shell contains an ideal compressible fluid which flows at a velocity U. The shell is acted upon by hydrostatic fluid pressure p. It is necessary to find the flow velocity at which the unperturbed shape of the previously loaded shell becomes unstable.

Using the classical shell theory based on the Kirchhoff–Love hypotheses, we can write the strain vector components in the curvilinear coordinates (α_1, α_2, z) as follows [7]:

$$\varepsilon_{11} = E_{11} + zk_{11}, \qquad \varepsilon_{22} = E_{22} + zk_{22}, \qquad \varepsilon_{12} = E_{12} + zk_{12}. \tag{1}$$

Here

$$\begin{gathered} E_{11} = \varepsilon_1 + (\varepsilon_1^2 + \omega_1^2 + \theta_1^2)/2, \qquad E_{12} = \omega_1 + \omega_2 + \varepsilon_1\omega_2 + \varepsilon_2\omega_1 + \theta_1\theta_2, \\ k_{11} = k_1 + \varepsilon_1 k_1 + \omega_1\tau, \qquad k_{12} = 2\tau + \tau(\varepsilon_1 + \varepsilon_2) + \omega_1 k_1 + \omega_2 k_2; \end{gathered} \tag{2}$$

$$\varepsilon_1 = u' + \psi_1 v + r_1 w, \quad \omega_1 = v' + \psi_1 u, \quad \theta_1 = w' - r_1 u, \quad k_1 = \theta_1' + \psi_1\theta_2, \quad \tau = t_1 + t_2,$$

$$t_1 = \theta_2' + \psi_1\theta_1, \quad (\,\cdot\,)' = \frac{1}{A_1}\frac{\partial(\,\cdot\,)}{\partial\alpha_1}, \quad r_1 = \frac{1}{R_1} \quad (1 \rightleftarrows 2), \quad \psi_1 = 0, \quad \psi_2 = \frac{A_2'}{A_2},$$

u, v, and w are the meridional, circumferential, and normal components of the displacement vector, θ_i are the angles of rotation of the undeformed normal, R_i are the principal curvature radii, and A_i are Lamé parameters; the notation $1 \rightleftarrows 2$ indicates the presence of equations and relations obtained from the previous ones by replacement of subscript 1 by 2 and subscript 2 by 1.

The shell strain components (2) can be written in matrix form

$$\varepsilon = \varepsilon_* + Ee/2. \tag{3}$$

Here $\varepsilon = \{E_{11}, E_{22}, E_{12}, k_{11}, k_{22}, k_{12}\}^{\mathrm{t}}$, $\varepsilon_* = \{\varepsilon_1, \varepsilon_2, \omega_1 + \omega_2, k_1, k_2, 2\tau\}^{\mathrm{t}}$ is the linear part of the strain, $e = \{\varepsilon_1, \varepsilon_2, \omega_1, \omega_2, \theta_1, \theta_2, k_1, k_2, \tau\}^{\mathrm{t}}$, and E is the matrix of linear factors.

The elastic relations can also be written in matrix form

$$T = \{T_{11}, T_{22}, T_{12}, M_{11}, M_{22}, M_{12}\}^{\mathrm{t}} = D\varepsilon. \tag{4}$$

Here T is the force and moment vector and D is the stiffness matrix. The matrices E and D have the form

$$E = \begin{bmatrix} \varepsilon_1 & 0 & \omega_1 & 0 & \theta_1 & 0 & 0 & 0 & 0 \\ 0 & \varepsilon_2 & 0 & \omega_2 & 0 & \theta_2 & 0 & 0 & 0 \\ \omega_2 & \omega_1 & \varepsilon_2 & \varepsilon_1 & \theta_2 & \theta_1 & 0 & 0 & 0 \\ k_1 & 0 & \tau & 0 & 0 & 0 & \varepsilon_1 & 0 & \omega_1 \\ 0 & k_2 & 0 & \tau & 0 & 0 & 0 & \varepsilon_2 & \omega_2 \\ \tau & \tau & k_1 & k_2 & 0 & 0 & \omega_1 & \omega_2 & \varepsilon_1 + \varepsilon_2 \end{bmatrix}, \quad D = \begin{bmatrix} a_{11} & a_{12} & 0 & b_{11} & b_{12} & 0 \\ a_{12} & a_{22} & 0 & b_{12} & b_{22} & 0 \\ 0 & 0 & a_{44} & 0 & 0 & b_{44} \\ b_{11} & b_{12} & 0 & c_{11} & c_{12} & 0 \\ b_{12} & b_{22} & 0 & c_{12} & c_{22} & 0 \\ 0 & 0 & b_{44} & 0 & 0 & c_{44} \end{bmatrix}.$$

In the stiffens matrix D, the coefficients are defined as

$$(a_{ij}, b_{ij}, c_{ij}) = \int_h (1, z, z^2) B_{ij}\, dz \qquad (i, j = 1, 2, 4)$$

(B_{ij} are the known coefficients included in Hooke's law for an isotropic material).

For a mathematical formulation of the problem, we use the principle of possible displacements supplemented with the work of inertia forces, which can be written in matrix form as

$$\int_S \delta\varepsilon^{\mathrm{t}}\, T\, dS + \int_V \delta d^{\,\mathrm{t}}\, \rho_m \ddot{d}\, dV - \int_S \delta d^{\,\mathrm{t}}\, P\, dS = 0. \tag{5}$$

Here ε, T, d, and P are the vectors of the generalized strains, generalized forces and the moments, displacements, and surface loads, respectively and ρ_m is the specific density of the shell material.

Let us consider the initial state of equilibrium determined by the displacement vector d^0, the strain vector ε^0, etc. The quantities characterizing the states with small deviations from the state of equilibrium can be represented as $d = d^0 + d^1$, etc. Then, in view of relations (3) and (4) and the assumptions of linearity of the initial equilibrium state, the vectors of the strain, strain variations, forces, and moments are written as follows:

$$\varepsilon = \varepsilon_*^0 + \varepsilon_*^1 + E^0 e^1 + E^1 e^1/2,$$

$$\delta\varepsilon = \delta\varepsilon_*^1 + E^0 \delta e^1 + E^1 \delta e^1, \qquad T = T^0 + T^1 + T^2, \tag{6}$$

$$T^0 = D\varepsilon_*^0, \qquad T^1 = D(\varepsilon_*^1 + E^0 e^1), \qquad T^2 = DE^1 e^1/2.$$

Substituting relations (6) into (5) subject to the initial condition, omitting terms of the third and fourth order of smallness, and performing simple transformations, we obtain the equilibrium condition for a state close to the initial state:

$$\int\limits_S \delta(\varepsilon_*^1)^{\mathrm{t}}\, D\varepsilon_*^1\, dS + \int\limits_V \delta(d^1)^{\mathrm{t}}\, \rho_m \ddot{d}^1\, dV - \int\limits_S \delta(d^1)^{\mathrm{t}}\, P^1\, dS + \int\limits_S \delta(e^1)^{\mathrm{t}}\, \sigma_0 e^1\, dS$$

$$+ \int\limits_S \delta(\varepsilon_*^1)^{\mathrm{t}}\, DE^0 e^1\, dS + \int\limits_S \delta(e^1)^{\mathrm{t}}\, DE^0 \varepsilon_*^1\, dS = 0. \tag{7}$$

Here the matrix σ_0, whose elements are found from the condition $(E^1)^{\mathrm{t}} D\varepsilon_*^0 = \sigma_0 e^1$ (the vector ε_*^0 is a solution of the corresponding static problem), is written as

$$\sigma_0 = \begin{bmatrix} T_{11} & 0 & 0 & T_{12} & 0 & 0 & M_{11} & 0 & M_{12} \\ 0 & T_{22} & T_{12} & 0 & 0 & 0 & 0 & M_{22} & M_{12} \\ 0 & T_{12} & T_{11} & 0 & 0 & 0 & M_{12} & 0 & M_{11} \\ T_{12} & 0 & 0 & T_{22} & 0 & 0 & 0 & M_{12} & M_{22} \\ 0 & 0 & 0 & 0 & T_{11} & T_{12} & 0 & 0 & 0 \\ 0 & 0 & 0 & 0 & T_{12} & T_{22} & 0 & 0 & 0 \\ M_{11} & 0 & M_{12} & 0 & 0 & 0 & 0 & 0 & 0 \\ 0 & M_{22} & 0 & M_{12} & 0 & 0 & 0 & 0 & 0 \\ M_{12} & M_{12} & M_{11} & M_{22} & 0 & 0 & 0 & 0 & 0 \end{bmatrix}.$$

In the examples presented below, the last two integrals in (7) are not considered, which corresponds to the hypothesis of a stressed undeformed state.

2. Equations of Motion for the Fluid and Numerical Implementation of the Problem. In the case of potential flow, the motion of an ideal compressible fluid occupying volume V_f in the shell is described by the wave equation, which, in cylindrical coordinates (r, θ, x), is written as follows [8]:

$$\nabla^2\phi = \frac{\partial^2\phi}{\partial r^2} + \frac{1}{r^2}\frac{\partial^2\phi}{\partial\theta^2} + \frac{\partial^2\phi}{\partial x^2} + \frac{1}{r}\frac{\partial\phi}{\partial r} = \frac{1}{c^2}\Big(\frac{\partial}{\partial t} + U\frac{\partial}{\partial x}\Big)^2\phi \tag{8}$$

(ϕ is the velocity perturbation potential and c is the sound velocity in the fluid). The fluid pressure P_f on an elastic structure ($S_\sigma = S_f \cap S_s$) is calculated by the linearized Bernoulli formula

$$P_f = p - \rho_f\Big(\frac{\partial\phi}{\partial t} + U\frac{\partial\phi}{\partial s}\Big). \tag{9}$$

Here ρ_f is the specific fluid density, s is the meridional coordinate of the shell, and S_f and S_s are the areas of the surfaces that bound the volumes of the fluid and shell, respectively. At the shell–fluid interface S_σ, we specify the nonpenetration condition

$$\frac{\partial\phi}{\partial n} = \frac{\partial w}{\partial t} + U\frac{\partial w}{\partial s}, \tag{10}$$

where n is the normal to the surface. At the entrance to and exit from the shell, the velocity perturbation potential obeys the boundary conditions

$$x = 0: \quad \phi = 0, \qquad x = L: \quad \frac{\partial\phi}{\partial x} = 0. \tag{11}$$

Applying the Galerkin method to the partial differential equation for the velocity perturbation potential (8) with boundary conditions (10) and (11), we obtain the integral relation [9]

$$\sum_{l=1}^{m_\phi}\Big[\int\limits_{V_f}\Big(\frac{\partial F_l}{\partial r}\,\frac{\partial F_k}{\partial r}+\frac{1}{r^2}\,\frac{\partial F_l}{\partial\theta}\,\frac{\partial F_k}{\partial\theta}+(1-\mathrm{M}^2)\,\frac{\partial F_l}{\partial x}\,\frac{\partial F_k}{\partial x}\Big)dV\Big]\phi_{al}$$

$$+\sum_{l=1}^{m_\phi}\Big(\int\limits_{V_f}\frac{2U}{c^2}\,\frac{\partial F_l}{\partial x}\,F_k\,dV\Big)\dot\phi_{al}+\sum_{l=1}^{m_\phi}\Big(\int\limits_{V_f}\frac{1}{c^2}\,F_lF_k\,dV\Big)\ddot\phi_{al}$$

$$-\sum_{i=1}^{m_s}\Big(\int\limits_{S_\sigma}N_i^wF_k\,dS\Big)\dot w_{ai}-\sum_{i=1}^{m_s}\Big(\int\limits_{S_\sigma}U\,\frac{\partial N_i^w}{\partial s}\,F_k dS\Big)w_{ai}=0,\quad k=1,m_\phi.$$

Here m_ϕ and m_s are the numbers of finite elements in the regions occupied by the fluid (V_f) and the shell (V_s), respectively, ϕ_{al} and w_{ai} are the nodal values for the fluid and shells, respectively, $\mathrm{M}=U/c$ is the Mach number, F and N_i^w are shape functions for the velocity perturbation potential and the normal component of the displacement vector.

The resulting equation can be written in matrix form

$$(K_\phi-A_\phi^c)\phi_a+M_\phi\ddot\phi_a-C_\phi^c\dot\phi_a-C_\phi w_a-A_\phi w_a=0, \tag{12}$$

where

$$K_\phi=\sum_{m_\phi}\int\limits_{V_f}\Big(\frac{\partial F^{\mathrm{t}}}{\partial r}\,\frac{\partial F}{\partial r}+\frac{1}{r^2}\,\frac{\partial F^{\mathrm{t}}}{\partial\theta}\,\frac{\partial F}{\partial\theta}+\frac{\partial F^{\mathrm{t}}}{\partial x}\,\frac{\partial F}{\partial x}\Big)\,dV,\qquad M_\phi=\sum_{m_\phi}\int\limits_{V_f}\frac{1}{c^2}\,F^{\mathrm{t}}F\,dV,$$

$$C_\phi=\sum_{m_s}\int\limits_{S_\sigma}F^{\mathrm{t}}N_w\,dS,\qquad C_\phi^c=-\sum_{m_\phi}\int\limits_{V_f}\frac{2U}{c^2}\,\frac{\partial F^{\mathrm{t}}}{\partial x}\,F\,dV,$$

$$A_\phi=\sum_{m_s}\int\limits_{S_\sigma}UF^{\mathrm{t}}\,\frac{\partial N_w}{\partial s}\,dS,\qquad A_\phi^c=\sum_{m_\phi}\int\limits_{V_f}\mathrm{M}^2\,\frac{\partial F^{\mathrm{t}}}{\partial s}\,\frac{\partial F}{\partial s}\,dV.$$

Using the standard procedures of the finite- element method for Eq. (7) and taking into account Eq. (9), we obtain the matrix relation

$$(K_s+K_g)d+M_s\ddot d+\rho_fC_\phi^{\mathrm{t}}\dot\phi_a+\rho_fA_s\phi_a=0. \tag{13}$$

Here $K_s=\sum\limits_{m_s}\int\limits_{S_s}B^{\mathrm{t}}DB\,dS$, B is the coupling matrix of the strain vector ε_* to the nodal displacement vector of the shell finite element, $K_g=\sum\limits_{m_s}\int\limits_{S_s}G^{\mathrm{t}}\sigma_0G\,dS$ is the geometrical stiffness matrix, G is the coupling matrix of the strains e to the nodal displacement vector, $M_s=\sum\limits_{m_s}\int\limits_{V_s}N^{\mathrm{t}}\rho_mN\,dV$, N is the matrix of the shape functions of the shell finite element, and $A_s=\sum\limits_{m_s}\int\limits_{S_\sigma}UN_w^{\mathrm{t}}\,\dfrac{\partial F}{\partial s}\,dS$.

The investigation of dynamic behavior of loaded shells of revolution with internal fluid flow reduces to the joint solution of two systems of equations (12) and (13). The combined system of equations can be written as

$$K\left\{\begin{array}{c}d\\ \phi_a\end{array}\right\}+M\left\{\begin{array}{c}\ddot d\\ \ddot\phi_a\end{array}\right\}+\rho_fC\left\{\begin{array}{c}\dot d\\ \dot\phi_a\end{array}\right\}+\rho_fA\left\{\begin{array}{c}d\\ \phi_a\end{array}\right\}=0,$$

where K is the stiffness matrix, M is the mass matrix, C is the damping matrix, and A is the aerodynamic stiffness matrix:

$$K=\left[\begin{array}{cc}K_s+K_g & 0\\ 0 & -\rho_fK_\phi\end{array}\right],\qquad M=\left[\begin{array}{cc}M_s & 0\\ 0 & -\rho_fM_\phi\end{array}\right],$$

$$C = \begin{bmatrix} 0 & C_\phi^{\mathrm{t}} \\ C_\phi & C_\phi^c \end{bmatrix}, \qquad A = \begin{bmatrix} 0 & A_s \\ A_\phi & A_\phi^c \end{bmatrix}.$$

Writing the expressions for the perturbed motion of the shell and fluid as

$$d = q \exp(i^* \lambda t), \qquad \phi_a = \phi \exp(i^* \lambda t),$$

where q and ϕ are some functions of the coordinates; $i^* = \sqrt{-1}$ and $\lambda = \lambda_1 + i^* \lambda_2$ is the characteristic parameter, we finally obtain

$$(K - \lambda^2 M + i^* \lambda \rho_f C + \rho_f A) \begin{Bmatrix} q \\ \phi \end{Bmatrix} = 0. \tag{14}$$

The solution of the problem of the dynamic behavior of loaded shells of revolution filled with a fluid reduces to the calculation and analysis of the eigenvalues λ of system (14). For a stationary fluid ($A = C_\phi^c = 0$), the eigenvalues of system (14) are real. For flow velocities $U > 0$, the eigenvalues of system (14) are complex or real, depending on the boundary conditions for the shell. When the flow velocity in the shell–fluid system reaches certain critical values, two types of instability are possible — static (divergence) and dynamic (flutter) — depending on the boundary conditions for the shell. In the case of instability of the first type, one of the eigenvalues has zero real part λ_1. In the case of instability of the second type, two vibration modes merge and one of the eigenvalues has a negative imaginary part λ_2.

The complex eigenvalues of system (14) are calculated using the Muller method (the parabola method) [10].

To perform a numerical implementation of the problem, we used a semi-analytical version of the finite-element method based on expanding the solution in a Fourier series in the circumferential coordinate θ. In this case, the initial two-dimensional problem reduces to a set of one-dimensional problems for each harmonic of the Fourier series.

For the shell, we used a finite element in the shape of a truncated cone with the meridional and circumferential displacement vector components approximated by a linear polynomial and the normal components approximated by a cubic polynomial. For the fluid, a triangular finite element with a linear approximation of the velocity perturbation potential was used.

The calculations were performed using 40 elements for the shell and 25 elements (along the radius) for the fluid, i.e., the total number of degrees of freedom was 718 (ignoring the boundary conditions).

3. Examples of Numerical Implementation. We consider vibrations of a conical shell (elastic modulus $E = 6.77 \cdot 10^{10}$ N/m^2, Poisson's ratio $\nu = 0.29$, $\rho_m = 2648$ kg/m^3, $R = 0.15$ m, $L = 0.56$ m, $h = 5.3 \cdot 10^{-4}$ m, and the cone angle is 15°) rigidly fixed at both ends and filled with a stationary fluid. Table 1 gives the lowest eigenfrequencies of vibrations f_0 for various harmonic numbers j. The results obtain in the present work are in good agreement with both numerical and experimental results (with an error not more than 2.5%) [11, 12].

Let us consider a rubber cylindrical shell rigidly fixed at two ends ($u = v = w = \partial w / \partial s = 0$) and filled with a moving gas treated as an incompressible medium. The calculations were performed for $L/R = 25.9$, $h/R = 0.0227$, $\rho_f / \rho_m = 0.001\,36$, $j = 2$, and $\nu = 0.5$. Figure 1 gives a curve of the first four dimensionless frequencies $\omega = \lambda / U_0$ versus the dimensionless flow velocity $\Lambda = U/U_0$, where $U_0 = \{E/[\rho_m(1-\nu^2)]\}^{1/2} = 36.73$.

Once flow velocity reaches the value $\Lambda_D = 0.601$, static instability (divergence) occurs, and for $\Lambda_F = 0.625$, flutter arises. At higher velocities, divergence for the third and fourth vibration modes takes place. The calculations results obtained in the present work are in good agreement with the results obtained in [13] using four terms of the Galerkin expansion only for the first three frequencies.

The dynamic behavior of cylindrical shells of revolution containing fluid flows has been investigated in a number of papers for various boundary conditions with the hydrostatic fluid pressure taken into account. It has been found that in the case of bilateral simple support [2] or clamping [3], divergence-type instability occurs, and in the case of a shell fixed at the end which is the entrance to the flow and free at the other end, flutter-type instability with one degree of freedom takes place [3]. In addition, the possibility of aerodynamic damping at subcritical velocities with asymmetric fastening of shells is discussed in [14, 15].

In the present work, we also performed calculations for a cylindrical shell under asymmetric boundary conditions, in particular, for a shell simply supported at one end ($v = w = 0$ at $x = 0$) and rigidly fixed at the other end. In this case, the parameters had the following values: $\nu = 0.3$, $L = 6.7$, $\mu = \rho_f R/(\rho_m h) = 3.21$, $k = h^2/(12R^2) = 1.51 \cdot 10^{-7}$, and $P = pR/(Eh) = 5.2 \cdot 10^{-6}$.

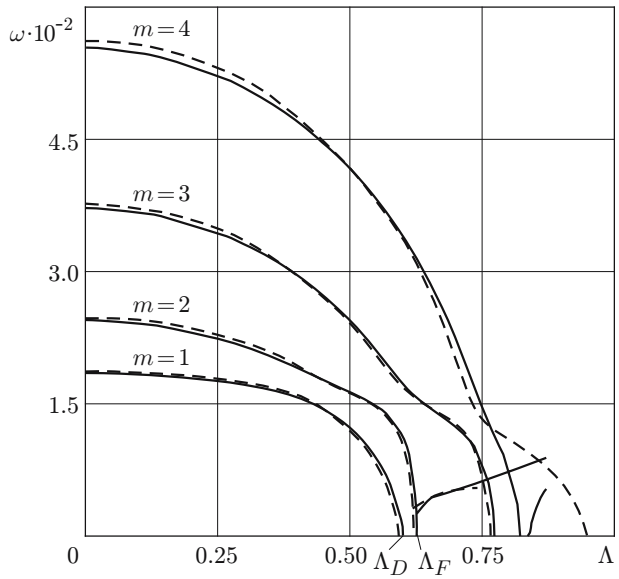

Fig. 1. Dimensionless eigenvalues ω versus dimensionless air flow velocity Λ for a rubber shell rigidly fixed at two ends: the solid curves are the calculation results of the present work; the dashed curves are the calculation results of [13].

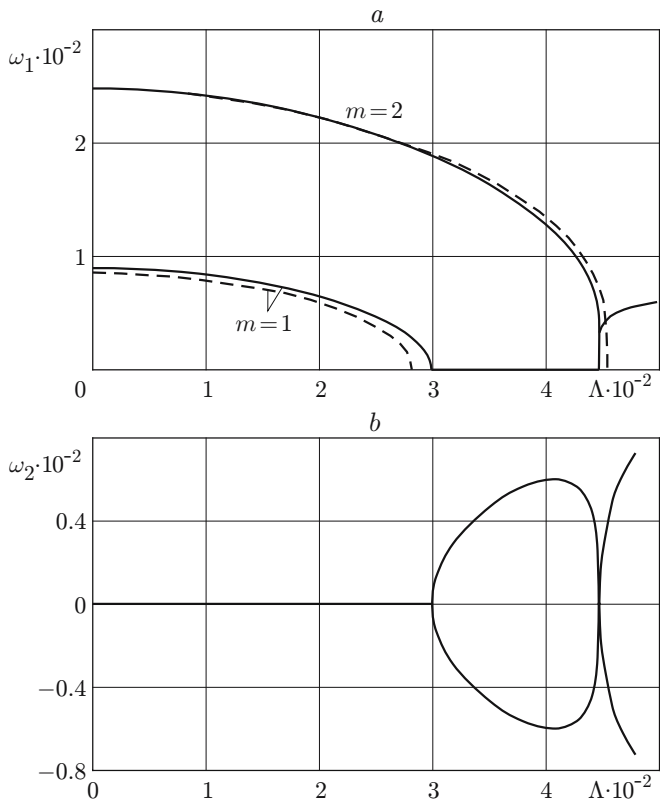

Fig. 2. Real (a) and imaginary (b) parts of the first two dimensionless eigenvalues versus dimensionless fluid velocity Λ for a cylindrical shell simply supported at one end and rigidly fixed at the other end: the solid curves are the calculation results of the present work; the dashed curves are the calculation results of [14].

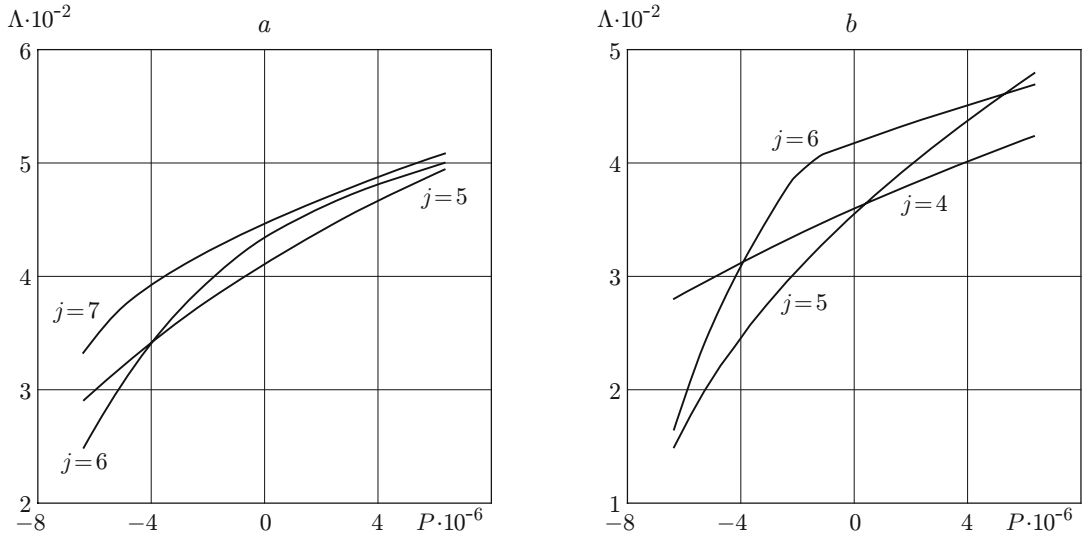

Fig. 3. Dimensionless critical divergence velocity Λ versus dimensionless static pressure P: (a) shell simply supported at one end face and rigidly fixed at the other end; (b) shell simply supported at both ends.

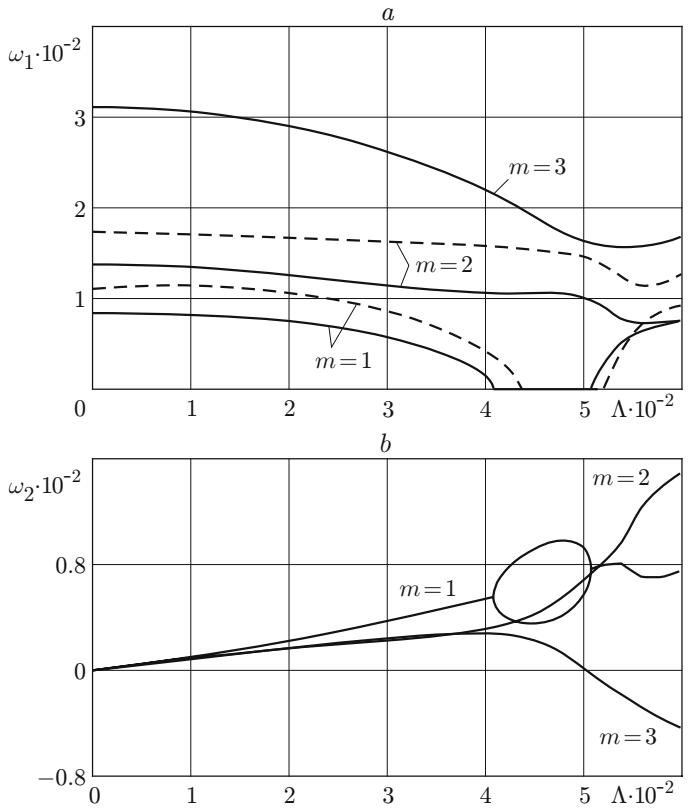

Fig. 4. Real (a) and imaginary (b) parts of the first three dimensionless eigenvalues versus dimensionless fluid velocity Λ for a cylindrical shell rigidly fixed at one ends and free at the other: the continuous curves are the calculations results of the present work; the dashed curves are the calculation results of [14].

TABLE 1

Eigenfrequencies of a Conical Shell Filled with an Incompressible Fluid for Various Hydrostatic Pressures

j	f_0, Hz			
	Calculation results of the present work	Calculation results of [11]	Calculation results of [12]	Experimental data of [12]]
		$p = 0$		
3	100.86	96.34	101.0	100.0
4	78.70	75.50	78.7	76.0
5	63.55	61.07	63.6	—
6	54.23	53.22	54.4	—
7	50.52	50.12	50.8	51.0
8	52.24	52.14	52.8	54.0
9	58.20	58.21	—	—
		$p = 0.1$ atm		
3	101.48	96.95	101.8	100.6
4	80.70	77.50	80.9	80.0
5	68.38	66.41	68.5	70.0
6	63.62	62.42	63.7	65.2
7	65.52	64.62	65.5	67.0
8	72.47	71.57	72.4	74.4
9	82.51	81.52	—	—
		$p = 0.3$ atm		
3	102.70	98.14	103.0	101.0
4	84.53	81.33	84.7	83.7
5	77.08	75.03	77.2	79.0
6	78.97	77.44	78.8	80.7
7	87.73	86.18	87.3	89.2
8	100.61	98.82	99.7	102.8
9	115.60	113.60	—	—
		$p = 0.5$ atm		
3	103.90	99.31	104.3	101.0
4	88.18	84.97	88.4	87.0
5	84.85	82.70	84.9	86.0
6	91.61	89.79	91.3	93.0
7	104.94	102.90	104.1	106.5
8	121.72	119.33	120.3	123.5
9	140.35	137.63	—	—

Figure 2 shows curves of the first two dimensionless frequencies $\omega = \lambda R/U_0$ [$\omega_1 = \mathrm{Re}\,(\omega)$, $\omega_2 = \mathrm{Im}\,(\omega)$, and $U_0 = (E/\rho_m)^{1/2}$] versus dimensionless velocity $\Lambda = U/U_0$ for $j = 6$. The real parts of the eigenvalues obtained in the present work are in good agreement with the calculation results of [14]. In [14], aerodynamic damping (in the subcritical region $\omega_2 \neq 0$) was found to occur under asymmetric boundary conditions. The results of the present work do not support the occurrence of aerodynamic damping in the range of subcritical velocities under the symmetric and asymmetric boundary conditions considered.

To compare the boundaries of instability for shells under symmetric and asymmetric boundary conditions, we studied the influence of static pressure on the dynamic characteristics of the system considered. Figure 3 shows the behavior of shells under various boundary conditions. It is evident that the type of instability depends on the pressure direction.

As noted above, for cantilever support of the shell, flutter-type instability with one degree of freedom occurs and aerodynamic damping is observed at $\Lambda > 0$. In addition, in [14], it was found that for the first vibration mode at $\omega_1 = 0$, two values $\omega_2 > 0$ exist. The calculations for $P = 3.1 \cdot 10^{-6}$ confirm the unusual dynamic behavior of the shell–fluid system (Fig. 4). The indicated feature is also observed for other pressure values and in its absence.

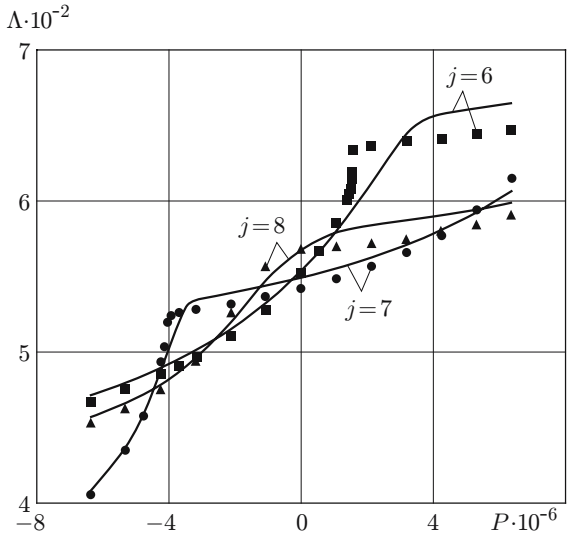

Fig. 5. Dimensionless critical flutter velocity Λ versus dimensionless static pressure P for a shell rigidly fixed at one end and free at the other: the solid curves refer to incompressible gas and the points refer to compressible gas.

The calculations for a cantilever supported shell show that the nature of instability depends significantly on the static pressure and the direction of its action (Fig. 5). In this problem, we estimated the effect of the gas compressibility ($c/U_0 = 0.0651$) on the position and shape of the boundary of instability, which as shown by the calculations, can be both stabilizing and destabilizing. In the case of critical harmonic numbers, the gas compressibility has only a destabilizing effect. It should be noted that the most significant difference between the results obtained taking into account and ignoring compressibility is observed only at high gas flow velocities ($M \gtrsim 1$).

Conclusions. The problem of the dynamic behavior of previously loaded shells of revolution containing a stationary or moving compressible fluid was formulated mathematically, and a finite-element algorithm for its numerical implementation was presented. The reliability of the algorithm was proved by a number of examples. A series of calculations was performed to study the influence of boundary conditions, static pressure, and gas compressibility on the dynamic behavior of the system modeled. A number of new data were obtained on the nature of instability of shells interacting with an internal liquid (gas) flow.

REFERENCES

1. M. P. Paidoussis and G. X. Li, "Pipes conveying fluid: A model dynamical problem," *J. Fluids Struct.*, **7**, No. 2, 137–204 (1993).
2. D. S Weaver and T. E. Unny, "On the dynamic stability of fluid conveying pipes," *J. Appl. Mech.*, **40**, 48–52 (1973).
3. M. P. Paidoussis and J.-P. Denise, "Flutter of thin cylindrical shells conveying fluid," *J. Sound Vibr.*, **20**, No. 1, 9–26 (1972).
4. J. Kochupillai, N. Ganesan, and C. Padmanabhan, "A semi-analytical coupled finite element formulation for shells conveying fluids," *Comput. Struct.*, **80**, 271–286 (2002).
5. Y. L. Zhang, D. G. Gorman, and J. M. Reese, "Vibration of prestressed thin cylindrical shells conveying fluid," *Thin-Walled Struct.*, **41**, 1103–1127 (2003).
6. Y. L. Zhang, J. M. Reese, and D. G. Gorman, "Finite element analysis of the vibratory characteristics of cylindrical shells conveying fluid," *Comput. Methods Appl. Mech. Eng.*, **191**, 5207–5231 (2002).
7. G. A. Vanin, N. P. Semenyuk, and R. F. Emel'yanov, *Stability of Shells Made of Reinforced Materials* [in Russian], Naukova Dumka, Kiev (1978).
8. A. S. Vol'mir, *Shells in Liquid and Gas Flow. Problems of Hydroelasticity* [in Russian], Nauka, Moscow (1979).

9. S. A. Bochkarev, "Finite-element analysis of the dynamic behavior of a cylindrical shell conveying a liquid," in: *Computational Mechanics* (collected scientific papers) [in Russian], No. 5, Izd. Perm. Gos. Tekh. Univ., Perm', (2006), pp. 9–20.
10. I. P. Zhidkov, *Computational Methods* [in Russian], Vol. 1, Nauka, Moscow (1966).
11. V. G. Grigor'ev, "Methodology of investigation of the dynamic properties of complex elastic and hydroelastic systems," Doct. Dissertation in Tech. Sci, Moscow (2000).
12. Yu. A. Gorbunov, L. M. Novokhatskaya, and V. P. Shmakov, "Theoretical and experimental study of the spectrum of natural axisymmetric vibrations of a conical shell containing a fluid in the presence of internal pressure," in: *Dynamics of Elastic and Solid Bodies Interacting with a Fluid* [in Russian], Izd. Tomsk Gos. Univ., Tomsk (1975), pp. 47–52.
13. M. P. Paidoussis and A. D. Mateescu, "Dynamics of cylindrical shell containing fluid flows with a developing boundary layer," *AIAA J.*, **25**, 857–863 (1987).
14. Ya. Gorachek and I. Zolotarev, "Influence of the fastening of the edges of a cylindrical shells containing fluid flow on the dynamic characteristics of the shell," *Prikl. Mekh.*, **20**, No. 8, 88–98 (1984).
15. M. P. Paidoussis, "Some unresolved issues in fluid-structure interactions," *J. Fluids Struct.*, **20**, No. 6, 871–890 (2005).